

## Sedimentation field flow fractionation monitoring of rice starch amylolysis

X. Morelon, S. Battu\*, C. Salesse, G. Begaud-Grimaud, D. Cledat, P.J.P. Cardot

*Laboratoire de Chimie Analytique et Bromatologie, Faculté de Pharmacie, Université de Limoges,  
2 rue du Dr Marcland, 87025 Limoges Cedex, France*

Received 17 December 2004; received in revised form 15 July 2005; accepted 19 July 2005

Available online 6 September 2005

### Abstract

Enzymatic starch granule hydrolysis is one of the most important reactions in many industrial processes. In this work, we investigated the capacity of SdFFF to monitor the native rice starch amylolysis. In order to determine if fractogram changes observed were correlated to granule biophysical modifications which occurred during amylolysis, SdFFF separation was associated with particle size distribution analysis. The results showed that SdFFF is an effective tool to monitor amylolysis of native rice starch. SdFFF analysis was a rapid (less than 10 min), simple and specific method to follow biophysical modifications of starch granules. These results suggested many different applications such as testing series of enzymes and starches. By using sub-population sorting, SdFFF could be also used to better understand starch hydrolysis mechanisms or starch granule structure.

© 2005 Elsevier B.V. All rights reserved.

*Keywords:* Sedimentation field flow fractionation; Native starch; Amylase

### 1. Introduction

Plants produce on the order of  $2 \times 10^{10}$  t/year of starch, providing 80% of the world's food calculated as calories. Starch are obtained from rice, wheat or maize as grain crops, and from potatoes, cassava or yam as tuber crops [1]. Most of the time, starch granules contain two polysaccharides: amylose and amylopectin. Amylose is defined as a linear molecule of (1 → 4) linked  $\alpha$ -D-glucopyranosyl units [2]. Amylopectine is the highly branched component of starch which is formed by chains of  $\alpha$ -D-glucopyranosyl units linked together mainly by (1 → 4) linkages but also with 5–6% of (1 → 6) bonds at the branched points [2,3]. The shape and size (1–100  $\mu$ m) of granules are characteristic of the botanical origin and vary from perfect spheres to polyhedral, rounded, or oval shapes [2,4]. Some starches such as some from potato or rice present a monomodal granule size distribution; while granules from wheat, or barley, for example, have a bimodal

particle size distribution with large A granules (10–40  $\mu$ m) and small B granules (1–10  $\mu$ m). Starch shape, size and size distribution plays a critical role in food fermentation processes [2,3]. Many studies report that large granules are more susceptible to chemical and enzymatic hydrolysis and are more useful in food chemistry [3,5–10]. Starch is hydrolyzed to glucose, maltose and malto-oligosaccharides by  $\alpha$ - or  $\beta$ -amylase and related enzymes. Amylases are the most important industrial enzymes widely used in different processes in food, textile or pharmaceutical industries [2,11–13]. Amylase does not easily hydrolyze native starch, and particularly starch without surface heterogeneity [2,3,10–13]. Nevertheless, because of the economic importance of amylolysis, and because of the interest in saving energy and water during industrial amylolysis [14], it was of major importance to study native starch enzymatic degradation, at low temperature, in order to optimize this process. Moreover, partially digested native starch, which appears as pitted or porous granules, could find useful applications in food, cosmetic or pharmaceutical industries [11]. Even though detailed information on cooked, gelatinized or damaged starch susceptibility to

\* Corresponding author. Tel.: +33 5 5543 5979; fax: +33 5 5543 5859.  
E-mail address: [battu@pharma.unilim.fr](mailto:battu@pharma.unilim.fr) (S. Battu).

amylolysis is available, data concerning native starch amylolysis are less numerous but increasing [8–12,14–20].

Field flow fractionation (FFF) was developed in the late 1960s by J.C. Giddings. This chromatographic-like separation family is described as one of the most versatile separation techniques [21,22]. The fundamental principle of FFF is based on the differential elution of species in a liquid (mobile phase) flowing through a ribbon-like capillary channel on a laminar mode [22]. Separation depends on specific particle susceptibility to an external field applied perpendicularly to the flow direction [22]. For sedimentation-FFF (SdFFF), also called centrifugal- or multigravitational-FFF, the external field applied is a multigravitational one, generated by the rotation of the separation channel in a complex device [22]. SdFFF is particularly well suited for isolation and characterization of micron-sized species such as starch by using the “Hyperlayer” elution mode. In this type of mechanism, granule size, density and shape are involved, as are channel geometry and flow rate characteristics [22–31]. In many recent works, FFF, SdFFF and Splitt technologies, have been successfully used to rapidly and easily analyze the particle size distribution of starch granules [5,6,32–40]. In this way, we have demonstrated the interest in combining information provided both by SdFFF (retention data) and flow cytometry (FC) (particle size distribution), in terms of size/density properties of a complex and polydispersed population such as yeast, cell lines or starch [40–42]. Recently, we described the interest of using SdFFF to monitor the induction of biological events (apoptosis and differentiation) in a cell line [43,44].

The use of SdFFF as a monitoring device for biological events is a new and interesting application. Therefore, we studied in this work, the capacity of SdFFF to monitor native rice starch amylolysis, a monomodal starch population (1–10  $\mu\text{m}$ ). Among native starches, native rice starch appeared to be efficiently attacked by  $\alpha$ - or  $\beta$ -amylase [12,16].

Starch enzymatic hydrolysis was characterized by optical microscopy, and by the reducing sugars release assay [11,12]. To determine if fractogram differences observed during amylolysis (shift of  $R_{\text{obs}}$  (void time versus retention time =  $t_0/t_r$ ), and peak shape changes) corresponded to biophysical granule changes which occur during amylolysis, SdFFF separation and collection of fraction were associated with particle size and particle size distribution analysis by flow cytometry [40–42].

The results showed that SdFFF is an effective tool to monitor amylolysis of native rice starch.

## 2. Materials and methods

### 2.1. Materials

Rice starch was purchased from Fluka (Sigma–Aldrich, Saint-Quentin Fallavier, France).  $\alpha$ -Amylase type VIII-A from barley (A-2771), sodium acetate, maltose, 3,5-

dinitrosalicylic acid and tartrate potassium were from Sigma–Aldrich (Sigma–Aldrich, Saint-Quentin Fallavier, France). Calcium chloride was from VWR International (VWR International SAS, Pessac, France).

### 2.2. Enzymatic hydrolysis

Starch samples were 3% (w/v) rice starch suspensions in acetate buffer pH 5.5 (0.02 M sodium acetate, 1 mM calcium chloride). Hydrolysis reactions were started by adding 2 units (as defined by Sigma–Aldrich) of  $\alpha$ -amylase/mg of starch to 20 mL starch samples. Assay and control (without amylase) starch samples were incubated at 35 °C with regular and gentle shaking. Reaction samples (assays and controls) were withdrawn at various time intervals (0–30 h incubation) and the enzymatic reaction was inactivated by lowering the pH to 2.0 with 1 M HCl. After agitation for 10 min, the mixture was neutralized with 1 M NaOH and centrifuged for 10 min at 3500 rpm. While the clear supernatant was removed and kept for the reducing sugar assay, the pellet containing starch granules was suspended in acetate buffer to obtain a 3% (w/v) suspension (crude population) which could be kept at 4 °C until SdFFF, flow cytometry and microscopic analyses (Leica DM LB optical microscope, Leica Microsystems, Reuil-Malmaison, France) were performed. The reducing sugar released into the reaction mixture (assay and control) was determined by a 3,5-dinitrosalicylic acid method [45]. The concentrations of reducing sugars were expressed according to the calibration curve for maltose.

### 2.3. SdFFF device and starch elution conditions

The SdFFF separation device used in this study has been previously described and schematized [46]. The separation channel was made up of two 930 mm  $\times$  40 mm  $\times$  2 mm polystyrene plates, separated by a Mylar<sup>®</sup> spacer in which the channel (817 mm  $\times$  13 mm  $\times$  0.175 mm with two V-shaped ends of 50 mm) was carved. The measured total void volumes were  $2058 \pm 10 \mu\text{L}$  ( $n=5$ ) which were calculated after injection and retention time determination (void time:  $t_0=0.588 \pm 0.050$  min) of an unretained compound (0.1 g/L of benzoic acid, UV detection at 254 nm). Inlet and outlet Peek<sup>®</sup> tubing (Upchurch Scientific, Oak Harbour, USA) were directly screwed to the accumulation wall. Then polystyrene plates and Mylar<sup>®</sup> spacers were sealed onto a centrifuge basket. The channel-rotor axis distance was measured at  $r=14.8$  cm. Sedimentation fields were expressed in units of gravity,  $1 g=980 \text{ cm/s}^2$ , and calculated as previously described [46]. A Waters 501 HPLC pump (Waters associate, Milford, MA, USA) was used to pump the sterile (autoclaved) mobile phase. A M71B4 Carpanelli engine associated with a pilot unit Mininvert 370 (Richards Systems, Les Ullis, France), controlled the rotating speed of the centrifuge basket. Sample injections were done by means of a Rheodyne<sup>®</sup> 7125i chromatographic injection device (Rheodyne, Cotati, CA, USA). Cleaning and decontamination

procedures have been described in a previous report [46]. The elution signal was recorded at 254 nm by means of a Spectroflow 783 programmable absorbance detector (ABI-Kratos, Ramsey, NJ, USA) and a 14-byte M1101 (100 mV input) acquisition device (Keithley Metrabyte, Tauton, MA, USA) operated at 2.2 Hz and connected to a Macintosh computer. The starch suspension elution conditions ranged from 7.5 to 15 g in external field strength and from 3.0 to 4.5 mL/min in mobile phase flow rate. The optimal elution conditions (“Hyperlayer” mode) have been experimentally determined and were: flow injection through the accumulation wall [47] of 25  $\mu$ l starch suspension (3%, w/v, acetate buffer pH 5.5), flow rate: 3.5 mL/min, mobile phase: sterile (autoclaved) distilled water; external multi-gravitational field strength:  $10.0 \pm 0.1$  g, spectrophotometric detection at  $\lambda = 254$  nm. Five fractions were collected in elution peaks from control and amylase digested starch: peak fractions 1–5 (PF<sub>*n*</sub>): PF<sub>1</sub>: 2 min 00 s/3 min 00 s; PF<sub>2</sub>: 3 min 00 s/3 min 50 s; PF<sub>3</sub>: 3 min 50 s/4 min 55 s; PF<sub>4</sub>: 4 min 55 s/6 min 00 s; PF<sub>5</sub>:/6 min 00 s/7 min 30 s. To obtain a sufficient quantity of starch for particle size analysis, we performed five successive SdFFF cumulative fraction collections.

#### 2.4. Flow cytometry

Flow cytometry versatility permits particle counting as well as measurements of particle characteristics using light scattering principles and/or fluorescence [48,49]. When a single particle passes in front of a laser beam, the scattered (or emitted fluorescence) light generates a signal dependent on the studied parameter of that particle. If the diffused light is collected at low angles (10°-forward scattering, FS) [48–50], diffraction predominates and the Mie Law [51] gives the dependence of scattered intensity on particle refractive index and geometrical cross-section, which is size and shape dependent. It is therefore possible to calibrate FC operated in the FS mode to obtain number versus size particle distribution histograms [40].

A flow cytometer EPICS-XL (Beckman Coulter France, Villepinte, France) with 1024 channels, equipped with an argon ion laser tuned to 488 nm at a beam power of 15 mW, was used for measurements. Flow-Check<sup>TM</sup> fluorospheres (Beckman Coulter France, Villepinte, France) were used to check the stability of the optical and fluid systems.

As previously described [40], polymer microsphere size standards (Duke Scientific, Palo Alto, CA, USA) of certified diameters were used for FS size calibration: refraction index of 1.59 at 589 nm at 23 °C (Duke Scientific Corporation) and nominal diameters of 3, 5 and 7  $\mu$ m (1.0% CV). These standards have a refractive index value very close to that of starch granules (1.54 at 25 °C) and were chosen to cover a size range including rice starch granule diameters [4]. The forward (FS) signal histograms were recorded at different gains. Flow cytometer software created Listmode files, which recorded cytometric data. WinMDI software ver. 2.8 (©Joseph Trotter) was used to transform data files into

the Excel format, in order to determine median channel value and associated data. This histogram used the overall FS signal intensity (1024 channels). From such a signal it was possible to calibrate the *x*-axis by means of certified average values of the latex standards. Mean diameter of every standard latex particle was plotted as a function of the corresponding FS median channel thereby establishing an FS calibration function. Calibrated size was a function of the logarithm of the flow cytometry FS channel number:

$$\text{diameter} = A \ln(\text{FS channel}) + B \quad (1)$$

This calibration equation was used to convert flow cytometry particle distribution into particle size distribution [40].

All samples: crude population and SdFFF fractions of the control starch or of the enzymatically hydrolyzed starch, were analyzed three times and data acquisition was stopped after 20,000 events were counted. For an FS amplification gain of 13.5, the equation used to determine the mean rice starch diameter was the following [40]:

$$\text{diameter} = 3.683 \ln(\text{FS mean channel}) - 18.038 \quad (2)$$

Thus, for all studied populations (crude and fractions) the mean starch diameter was determined. Then, they were used to establish histograms: mean diameter as a function of SdFFF fractions. This described the mean particle size distribution in the eluted population and allowed us to follow biophysical changes during starch amylolysis.

### 3. Results and discussion

#### 3.1. Rice starch SdFFF elution

First, in order to use SdFFF as a monitoring tool for amylolysis, we optimized starch elution conditions to obtain a reference profile. Different studies [5,6,35,37,40] have demonstrated that micron-sized particles, such as starches, could be eluted under two different elution modes: “Hyperlayer” and “Steric”. In the “Hyperlayer” mode, the flow velocity/channel thickness balance generates a hydrodynamic lift force which drives the particles away from the accumulation wall. Particles are then focused into a thin layer which corresponds to an equilibrium position in the channel thickness where the external field is exactly balanced by the hydrodynamic lift forces [22–31]. At this position, the risk of starch-wall interactions is negligible, providing better particle separation. At equivalent densities, the “Hyperlayer” elution mode predicts a size dependent particle elution order: large particles are eluted first; and at equivalent sizes, predict a density dependent elution order: denser particles are eluted last. The different average velocities of the different species are compared by means of the observed retention ratio  $R_{\text{obs}}$  which is the ratio of the void time versus the retention time  $= t_0/t_r$  [30]. If the external field can be increased sufficiently, or flow rate decreased sufficiently to offset lift forces, micron-sized

particles are confined to a very thin layer close to the accumulation wall. This elution mode is described as “Steric” [22–31] and appears as a limit case of “Hyperlayer”. By driving particles close to the accumulation wall, the “Steric” elution mode enhances particle/channel wall interactions which lead to channel poisoning with harmful consequences on repeatability, reproducibility and particle recovery [46]. Poisoning corresponds to all species such as starch, enzymes, fragments of hydrolyzed starches, microorganisms, etc., which could absorb on the channel wall, leading to modification of its surface characteristics, and in consequence, changing particle retention.

Thus, SdFFF elution conditions: flow injection of starch mixture; mobile phase flow rate: 3.5 mL/min; external field strength:  $10.00 \pm 0.01$  g; carrier phase composition (sterile distilled water) and polystyrene channel walls; were selected to promote the “Hyperlayer” elution mode in order to overcome granule-channel wall interactions, channel poisoning and microorganism contamination, in association with daily cleaning and decontamination procedures [46,47,52].

Fig. 1 shows a representative elution fractogram obtained for native rice starch (3%, w/v). Two major peaks were observed: the first corresponding to unretained species (void volume peak:  $R_{\text{obs}} \approx 1$ ), and the second ( $R_{\text{obs}} = 0.136 \pm 0.002$ ,  $n = 5$ ) corresponding to the starch granules. After total elution, the external field was stopped (ER, Fig. 1), and we observed a residual signal (RP, Fig. 1) which corresponded to particle release from the separating channel.

In the “Hyperlayer” elution mode, micron-sized species showed an  $R_{\text{obs}}$  that was flow rate and external field dependent [22–31]. At constant field, the increase in flow rate induces an increase in  $R_{\text{obs}}$ , and at constant flow the increase in field decreases  $R_{\text{obs}}$ . We measured the  $R_{\text{obs}}$  pattern of the specific elution peak for native rice starch under different

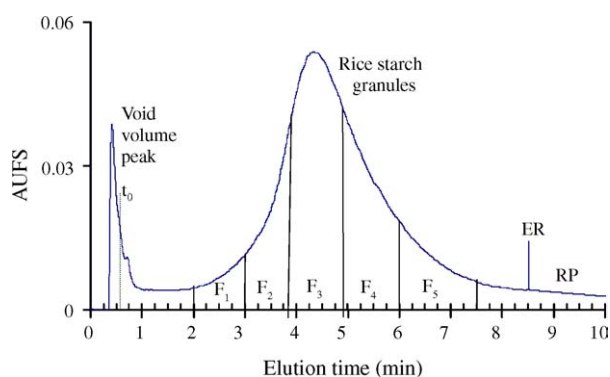


Fig. 1. Representative fractogram of native rice starch after SdFFF elution. *Elution conditions:* channel, 817 mm  $\times$  13 mm  $\times$  0.175 mm (polystyrene walls); flow injection of 25  $\mu$ L rice starch suspension (3%, w/v in 0.02 M acetate buffer pH 5.5); flow rate, 3.5 mL/min; mobile phase, sterile distilled water; external multigravitational field, 10 g; spectrophotometric detection at  $\lambda = 254$  nm. ER corresponds to the end of channel rotation, in this case the mean externally applied field strength was equal to zero gravity, thus RP, a residual signal, corresponds to the release peak of reversible particle-accumulation wall sticking. The void time ( $t_0$ ) was determined by independent injection of an unretained compound (0.1 g/L of benzoic acid).

elution conditions. At a constant field of  $10.0 \pm 0.1$  g, the increase in flow rate resulted in an increase in  $R_{\text{obs}}$ :  $R_{\text{obs}} = 0.127 \pm 0.004$  at 3.0 mL/min and  $R_{\text{obs}} = 0.144 \pm 0.006$  at 4.5 mL/min (mean  $\pm$  SD for  $n = 3$ ). A field increase at a constant flow rate (3.5 mL/min) resulted in a decrease in  $R_{\text{obs}}$  with  $R_{\text{obs}} = 0.166 \pm 0.002$  at 7.5 g and  $R_{\text{obs}} = 0.131 \pm 0.002$  at 15.0 g (mean  $\pm$  SD for  $n = 3$ ).

Secondly, in the “Hyperlayer” mode, particles are driven away from the accumulation wall. By using the following equation [27],

$$R = \frac{6s}{\omega} \quad (3)$$

in which  $R$  is the retention ratio,  $\omega$  the channel thickness (175  $\mu$ m), and  $s$  is the distance of the center of the focused zone from the channel wall [27]. We calculated the approximate average starch elevation ( $s$ ) using  $R_{\text{obs}}$  values ( $R_{\text{obs}} = 0.136 \pm 0.002$ ,  $n = 5$ ), and  $s = 3.97$   $\mu$ m. By using flow cytometer, the mean starch granule diameter was  $4.95 \pm 0.15$   $\mu$ m ( $n = 3$ ). Thus, as the estimated starch radius (2.48  $\mu$ m) was less than the approximate average granule elevation value ( $s = 3.97$   $\mu$ m), this confirmed starch elution by the “Hyperlayer” mode.

Finally, the effectiveness of this mode in reducing particle-accumulation wall interactions was shown in part by the low level of the corresponding release peak at the end of the fractogram (Fig. 1).

### 3.2. Amylolysis monitoring by SdFFF

Among native starches, rice starch is efficiently attacked by  $\alpha$ - or  $\beta$ -amylase [12,16]. Thus, we chose  $\alpha$ -amylase type VIII-A from barley (Sigma) which was a mixture of  $\alpha$ - and  $\beta$ -amylase, leading to a cooperative starch hydrolysis, even if  $\alpha$ -amylase activity appeared to be the more important to initialize and produce starch degradation [11,12]. Amylolysis was investigated by using the reducing sugar release and the microscopic aspect of the starch suspension. Table 1 shows the reducing sugar release, expressed in maltose, during

Table 1

Assay of reducing sugar release into the reaction mixture during native rice starch amylase hydrolysis

Incubation time (h)	Reducing sugar ( $\text{mol L}^{-1}$ )
0	
0.144 $\pm$ 0.002	
14	0.149 $\pm$ 0.004
20	0.162 $\pm$ 0.002
24	0.177 $\pm$ 0.002
30	0.177 $\pm$ 0.002

Assay was performed by using the Bernfield methods [45]. The concentrations of reducing sugars were expressed according to the calibration curve for maltose. Results are displayed as mean  $\pm$  SD for  $n = 3$ . During hydrolysis, a control sample was incubated and measured for reducing sugar in the same conditions as for the assay, and no reducing sugar were detected.



starch hydrolysis. In comparison to controls (no significant absorbance), we measured a significant increase in reducing sugar production associated with enzymatic hydrolysis. As previously described [18], we showed a relatively fast release initially (0–2 h), followed by a slower reaction until 30 h incubation. The modification of the starch granule population during hydrolysis is shown in Fig. 2. We observed a decrease in starch granule number with increasing incubation times, and a slight decrease in the apparent diameter of residual particles (Fig. 2b and c). This result, as well as those from the reducing sugar release assay, are proof of an enzymatic reaction [11,12,18].

Fig. 3 displays representative fractograms of native rice starch incubated with amylase; separations were performed under conditions defined above. First, we compared fractograms obtained for control rice starch after 0 and 30 h incubation (Fig. 3). They did not demonstrate important differences in peak shape or in retention time, leading to a comparable retention ratio as described in Table 2. This indicated that, in the absence of enzymatic activity, the incubation process (continuous mechanical stirring at 35 °C) did not modify biophysical properties of starch granules. Thus, changes observed in the presence of amylase could be linked to enzymatic activity (Table 1, Figs. 2 and 3).

In comparison to control rice starch, we observed during amylolysis, a marked change in SdFFF elution profiles concerning both retention times and retention ratio ( $R_{\text{obs}}$ , Table 2). According to the “Hyperlayer” elution mode description [22–31], retention changes indicated an evolution of mean starch granule biophysical properties (size, density or shape). The principal peak shape differences corresponded to a time dependent decrease in the starch peak signal, while the void volume signal increased, indicating both the decrease in starch granule number and the formation of small residues eluted in the void volume (Fig. 3). These results were correlated with those observed in Fig. 2 which showed a decrease in starch granule number.

As previously described [3,8–12,53,54], rice and other native starch amylolysis [12], starts by the absorption of amylase on a specific region of the granule surface. Then, the

Table 2  
Retention ratio  $R_{\text{obs}}$  changes during raw starch enzymatic hydrolysis

Sample (incubation time)	$R_{\text{obs}}$
Control rice starch (0 h)	0.136 ± 0.002
Control rice starch (30 h)	0.137 ± 0.004
Hydrolyzed rice	
2 h	0.123 ± 0.003
8 h	0.118 ± 0.002
20 h	0.117 ± 0.003
30 h	0.114 ± 0.004

Elution conditions: channel, 817 mm × 13 mm × 0.175 mm, flow injection of 25  $\mu\text{L}$  rice starch suspension (3%, w/v); flow rate, 3.5 mL/min; mobile phase, sterile distilled water; external field, 10 g; spectrophotometric detection at  $\lambda = 254$  nm. Results were expressed as mean  $\pm$  SD for  $n = 3$  (independent SdFFF separations).

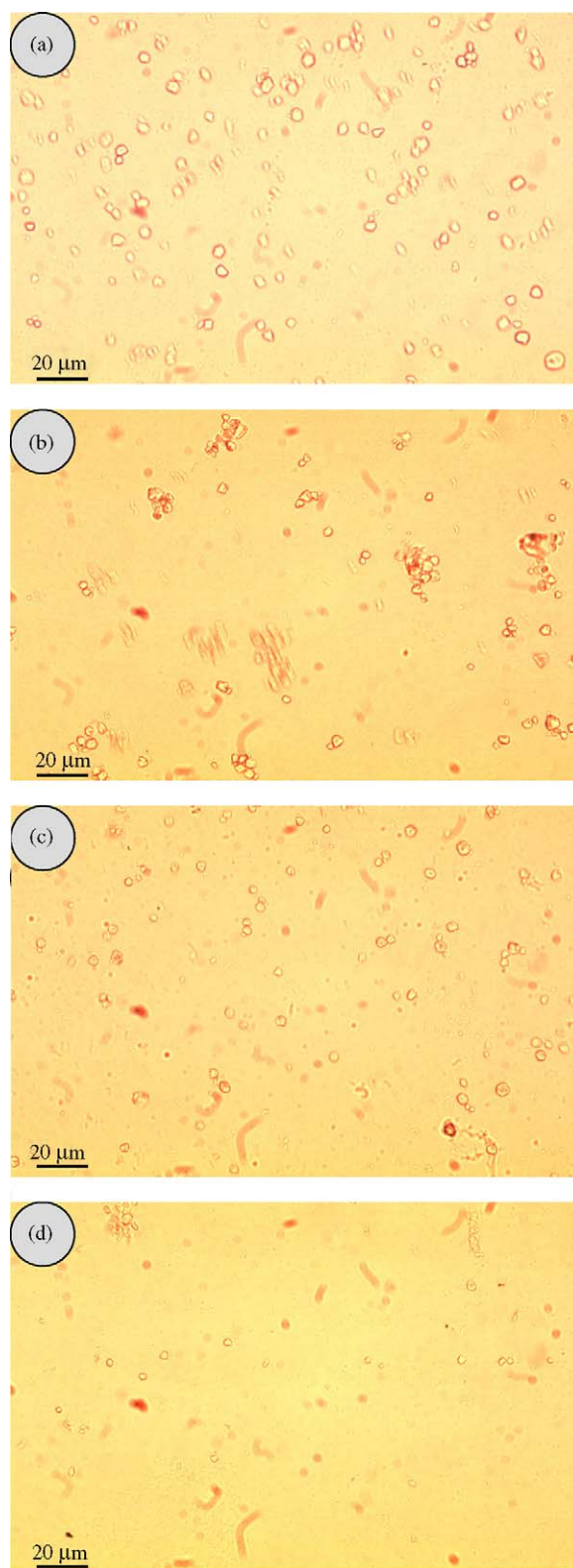


Fig. 2. Microscopic observation of rice starch. Rice starch suspension (3%, w/v starch suspension in 0.02 M acetate buffer, pH 5.5) was photographed by using a Leica DM LB optical microscope (Leica Microsystems, Reuil-Malmaison, France, magnification:  $\times 400$ ). (a) Crude rice starch; (b) rice starch incubated with amylase for 2 h (2 IU  $\alpha$ -amylase/mg starch); (c) rice starch incubated with amylase for 8 h; (d) rice starch incubated with amylase for 20 h.

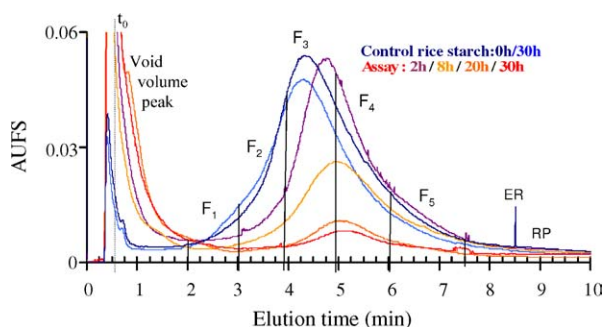


Fig. 3. SdFFF monitoring of native rice starch enzymatic hydrolysis after 2–30 h incubation. *Elution conditions:* channel, 817 mm  $\times$  13 mm  $\times$  0.175 mm (polystyrene walls), flow injection of 25  $\mu$ L rice starch suspension (control rice starch, 3%, w/v in 0.02 M acetate buffer pH 5.5/assays, 3%, w/v in 0.02 M acetate buffer pH 5.5 in the presence of 2 IU  $\alpha$ -amylase/mg starch); flow rate, 3.5 mL/min; mobile phase, sterile distilled water; external multigravitational field, 10 g; spectrophotometric detection at  $\lambda$  = 254 nm. ER corresponds to the end of channel rotation, in this case the mean externally applied field strength was equal to zero gravity, thus RP, a residual signal, corresponds to the release peak of reversible particle-accumulation wall sticking. The void time ( $t_0$ ) was determined by independent injection of an unretained compound (0.1 g/L of benzoic acid).

enzyme either digests channels toward the center of the granule (centripetal attack) or erodes the entire (or a section of the) granule surface (peripheral attack) [3,8–12,53,54]. The centripetal hydrolysis appears to be more specific to large granules ( $>10 \mu\text{m}$ ) [10,54]. In this mechanism, amylase first generates a few holes or pores, and then reaches the center of the granule by the formation of channels. Finally, the enzyme attacks the granule from the inside, leading to particle disruption and fragmentation [3,10,53,54]. In the case of small granules ( $<10 \mu\text{m}$ ), they are more specifically concerned by peripheral hydrolysis. Starches are hydrolyzed from the outside and have a rough surface. Surface erosion is followed by granule solubilization [10,54]. These processes are associated with reducing sugar release and starch structure modification and biophysical property changes (size, density

or shape). Amylolysis could be associated with a reduction in mean granule diameter [8,16].

Thus, enzymatic activity induces size, density or granule shape modifications which can be monitored by SdFFF elution. In order to investigate the relationship between SdFFF profile changes and enzymatic hydrolysis importance in biophysical starch properties modification, particle diameter and particle size distribution were studied.

### 3.3. Starch granule modification

The mean diameter of the starch granule population (control and hydrolyzed starches) was determined using a flow cytometer as described above [40]. The particle size distribution was analyzed in comparison to the crude population (Figs. 4 and 5), by measuring the mean population size of particles eluted in the fractions collected over time after SdFFF sorting (Figs. 1 and 3). The micron sized particle elution order was described, under the “Hyperlayer” elution mode, as being size, density and shape dependent [22–31]. By measuring the particle size distribution of eluted starch, we could more easily evaluate the respective influence of the two principal parameters which were size and density [40,43]. The effect of shape modification should not be neglected, but it appeared to be more difficult to evaluate its contribution to retention changes. The particle shape is reported to influence retention behavior either in the “Normal” or “Hyperlayer” mode [43,55–70]. The effect of shape is observed for irregular or nonspherical particles having a large aspect ratio (length/width) such as long rods and disks. In this case, the value of the diameter of nonspherical particle using FFF retention data and calibration curves (usually made with spherical standards) were different from the diameter of a sphere of the same volume. As a consequence, a difference between FFF results and other size measurement methods (Coulter counting, microscopy, . . .) is observed for nonspherical particles, in contrast to spherical ones [66–70]. In the “Steric” and “Hyperlayer” modes, the mean distance of

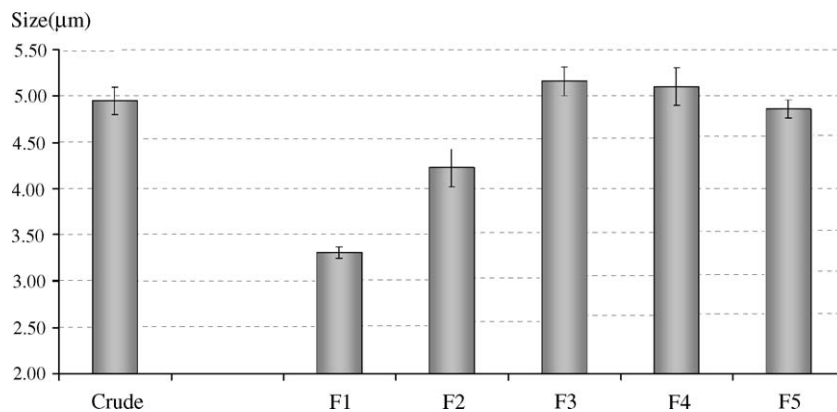


Fig. 4. Particle size distribution of control rice starch. The mean particle diameter was determined for a 3% (w/v) starch suspension (0.02 M acetate buffer pH 5.5) with calibrated EPICS XL flow cytometer (Beckman-Coulter) as described in Section 2. SdFFF elution and fraction collection were performed as described in Fig. 1. Results are displayed as mean  $\pm$  SD for  $n = 3$  (independent SdFFF separations).

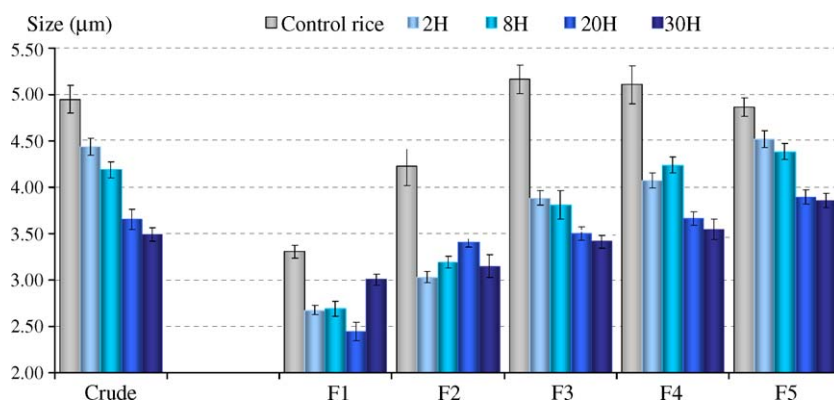


Fig. 5. Particle size distribution evolution of rice starch during amylolysis. The mean particle diameter (EPICS XL flow cytometer, Beckman-Coulter) was determined for a 3% (w/v) starch suspension (0.02 M acetate buffer pH 5.5) for control starch, and in the presence of 2 IU  $\alpha$ -amylase/mg for hydrolyzed starch for different incubation times (2, 8, 20 and 30 h). SdFFF elution and fraction collection were performed as described in Figs. 1 and 3. Results are displayed as mean  $\pm$  SD for  $n = 3$  (independent SdFFF separations).

the particle center of mass from the accumulation wall (which determine retention) will differ as the particle deviates from spherical shape. In “Steric” mode, the mean distance depends on particle motion [70]. Thus, rods may either roll along the wall or they may tumble end-over-end in response to shear forces [70]. Hydrodynamic forces also depend on particle shape. Nonspherical particles, such as disks, generate more lift-forces than spheres of the same volume and are eluted earlier [64,67,70]. Thus, nonspherical fly ash particle size distribution, determined by SdFFF, seems to be shifted to larger sizes compared with that one obtained by Coulter counting or microscopy [67]. Native rice consists of irregular granules (Fig. 2a) that could be eluted faster than perfect spheres of the same volume, as described for silica particles [64].

Fig. 4 shows the particle size distribution of control rice starch. The mean diameter of the crude population was  $4.95 \pm 0.15 \mu\text{m}$  ( $n = 3$ ), and this value appeared to be in the range of those previously described [4,40]. Using SdFFF elution and fraction collection, we observed a particular particle size distribution between the different fractions (Fig. 4). According to the “Hyperlayer” elution mode description, for a population having the same density, the large particles are eluted first. However, we observed (Fig. 4) an elution order reversed in size from fractions F1–F3 (small particles eluted first), while for the three last fractions (F3–F5), larger particles were eluted before the smaller one. Fractions F1–F3 had an elution order which suggested a density dependent elution mode. In agreement with the “Hyperlayer” elution mode description [22–31], we can state that particles eluted in F1 were less dense than F2 particles, and that F2 particles were less dense than particles eluted in F3. For the fraction F3 compared with fractions F4 and F5, we observed an elution of particles with probably equivalent density (Fig. 4).

These interesting results demonstrated the size and density polydispersity of the native starch population, suggesting the presence of starch granule populations of reduced size and density. Nevertheless, granule density also appeared to be dependent on water content [2]. Similar results have been also

reported with GFFF separation [37], for which small starch granules ( $4.63 \mu\text{m}$  diameter) were eluted in the void volume (under the weak earth’s gravitational field), before retained starch granules of  $5.04 \mu\text{m}$ . Contado et al. [37] suggested that this particular elution order might be due to the lower density of the first eluted particles. In our conditions, with a higher gravitational field (10 g), small granules were retained and eluted in the corresponding peak. Nevertheless, a complete study of the starch population diversity lies beyond the aim of this work.

Fig. 5 displayed the changes in particle size distribution during amylolysis, in comparison to a control population. For the crude starch population (Fig. 5), we observed a large decrease in mean granule size between 2 and 20 h. This effect was smaller after this time point. The size reduction can be also observed in Fig. 2b and c. According to the surface erosion model [10,54], we can suppose that the first effect of amylolysis would be particle size decrease. This phenomenon reflected enzymatic hydrolysis which could decrease mean particles diameter [8,16]. This could explain the retention time increase and  $R_{\text{obs}}$  reduction observed in fractograms (Fig. 3 and Table 2). The maximum decrease in  $R_{\text{obs}}$  was obtained after 2 or 8 h incubation. Over this time point,  $R_{\text{obs}}$  stayed relatively constant (Fig. 3, Table 2). A similar effect was seen for all SdFFF collected fractions (Fig. 5).

Two specific results should be emphasized. First, size reduction was less for the last fraction. After 2 h the diameter decreased 19% for F1, 25% for F3 and only 7% for F5. One explanation can be proposed. If the enzymatic attack decreased starch granule diameter, then, at constant density, the decrease in particle diameter led to an increase in retention time (“Hyperlayer” elution mode) (Table 2, Fig. 3). Thus, a particle initially eluted in fractions F3 or F4 (before amylolysis) could be eluted in fraction F5 during hydrolysis and diameter reduction. This could explain the lesser size decrease in F5 in comparison to other fractions (Fig. 5). We can also suppose, as described for starches with bimodal populations, that this result could be linked to the size dependent



susceptibility of starch granules to amylolysis [5–10]. Fig. 2 seems to demonstrate that large granules were preferentially attacked.

Second, Fig. 5 also shows an interesting phenomenon which corresponded to the relative increase in particle diameter in fractions F1 and F2 after 8 h incubation. As described [10,54], surface erosion was followed by granule solubilization. This suggests that, before total disruption and solubilization of the granule, this effect could be involved in an increase in water content and a decrease in granule density [2,10,54]. According to the “Hyperlayer” elution mode [22–31], the decrease in density led to a decreased retention time.

Thus, we can hypothesize different SdFFF elution steps of particles during amylolysis which is the result of a complex size/density evolution of the starch granules. In a first step of hydrolysis, we observed a reduction in particle diameter. As described above, large particles initially eluted in fraction F3 were then eluted in fractions F4 and F5 (Fig. 5). In a second step which associated diameter and density decrease, particles eluted in F5 fractions were then eluted in fractions F1 or F2, explaining the relative increase in particle diameter in these fractions (Fig. 5). These results emphasized the interest of coupling granule sorting by SdFFF with particle size distribution measurement and structural studies in order to explore amylolysis reactions and/or starch granule structure.

Finally, in our experimental conditions, with the exception of fraction F1 (Fig. 5), we only observed a slight size evolution after 20 h incubation. This result was correlated with the decrease in reducing sugar release (Table 1) which could reflect, as described [2,11,12], the presence of a amylolysis resistant starch granule population, observed in Fig. 2d.

Reducing sugar release assays, microscopic observation, as well as particle size distribution demonstrated the effectiveness of barley  $\alpha$ -amylase in hydrolyzing native starch samples in our experimental conditions. This led to important SdFFF elution profile differences. The coupling of SdFFF separation and particle size measurement could be an effective analytical tool to study the complex size/density evolution which occurs during amylolysis.

#### 4. Conclusion

As described in the literature, amylolysis results in a centripetal or peripheral attack of starch leading to important changes in granule structure associated with many biophysical property modifications (size, density, shape). It appeared that SdFFF elution profile changes could be linked to the enzymatic reaction.

As SdFFF takes advantage of intrinsic biophysical properties of starch, and because (1) no complex mobile phase, or sample preparations are needed, (2) elution is rapid (less than 10 min), and (3) the device can quickly and easily be set up for optimal elution, SdFFF proved, after acquisition of a reference profile, to be a fast, practical and specific method to monitor amylolysis of native starches. These results sug-

gested different applications such as screening series of enzymes, starches and enzymatic conditions. Moreover, as it was possible to collect time-dependent fractions containing granules having a narrow size range, SdFFF could be coupled to specific starch characterization tools such as particle size distribution measurement (Coulter Counter, Flow cytometer), X-ray diffraction pattern, electronic microscopy, in order to explore and better understand the specific mechanisms of amylolysis and/or starch granule structure.

#### Acknowledgements

The authors would like to thank NaBiPa-DAAD program (1999–2003) with Offenburg for technical and financial help. Part of this work (flow cytometry) was supported by a grant from Aide à la Recherche Régionale (Limousin 2002). Jeanne Cook-Moreau is deeply thanked for English and style corrections.

#### References

- [1] M. Sivak, J. Preiss, *Starch: Basic Science to Biotechnology*, Academic Press, New York, 1998.
- [2] A. Buleon, P. Colonna, V. Planchot, S. Ball, *Int. J. Bio. Macromol.* 23 (1998) 85.
- [3] J.R. Stark, A. Lynn, *Biochem. Soc. Trans.* 20 (1992) 7.
- [4] J.L. Jane, T. Kasemsuwan, S. Leas, H. Zobel, J.F. Robyt, *Starch/Stärke* 46 (1994) 121.
- [5] L. Farmakis, J. Sakellaraki, A. Koliadima, D. Gavril, G. Karaiskakis, *Starch/Stärke* 52 (2000) 275.
- [6] J. Janouskova, M. Budinska, J. Plockova, J. Chmelik, *J. Chromatogr. A* 914 (2001) 183.
- [7] P. Meredith, *Starch/Stärke* 33 (1981) 40.
- [8] M. Lauro, P.M. Forsell, M.T. Suortti, S.H.D. Hulleman, K.S. Poutanen, *Cereal Chem.* 76 (1999) 925.
- [9] P. Colonna, A. Buleon, F. Lemarie, *Biotechnol. Bioeng.* 31 (1988) 895.
- [10] C.M.L. Franco, C.F. Ciacco, *Starch/Stärke* 44 (1992) 422.
- [11] H.K. Sreenath, *Starch/Stärke* 44 (1992) 61.
- [12] E. Sarikaya, T. Higasa, M. Adachi, B. Mikami, *Process Biochem.* 35 (2000) 711.
- [13] P.M. Baldwin, M.C. Davies, C.D. Melia, *Int. J. Bio. Macromol.* 21 (1997) 103.
- [14] S.D. Textor, G.A. Hill, D.G. Macdonald, E. St Denis, *Can. J. Chem. Eng.* 76 (1998) 87.
- [15] W.J. Wang, A.D. Powell, C.G. Oates, *Carbohydr. Polym.* 26 (1995) 91.
- [16] T. Ohtani, T. Yoshio, S. Hagiwara, T. Maekawa, *Starch/Stärke* 52 (2000) 150.
- [17] C. Gerard, P. Colonna, A. Buleon, V. Planchot, *J. Sci. Food Agric.* 81 (2001) 1281.
- [18] H. Tang, K. Watanabe, T. Mitsunaga, *Carbohydr. Polym.* 49 (2002) 217.
- [19] C. Yook, J.F. Robyt, *Carbohydr. Res.* 337 (2002) 1113.
- [20] T. Matsubara, Y. Ben Ammar, T. Anindyawati, S. Yamamoto, K. Ito, M. Iizuka, N. Minamiura, *J. Biochem. Mol. Biol.* 37 (2004) 422.
- [21] J.C. Giddings, *Sep. Sci.* 1 (1966) 123.
- [22] J.C. Giddings, in: M.E. Schimpf, K. Caldwell, J.C. Giddings (Eds.), *Field-Flow Fractionation Handbook*, John Wiley & Sons Inc., New York, 2000, p. 3.



- [23] K.D. Caldwell, T.T. Nguyen, T.M. Murray, M.N. Myers, J.C. Giddings, *Sep. Sci. Technol.* 14 (1979) 935.
- [24] K.D. Caldwell, Z.Q. Cheng, P. Hradecky, J.C. Giddings, *Cell Biophys.* 6 (1984) 233.
- [25] K.D. Caldwell, in: M.E. Schimpf, K.D. Caldwell, J.C. Giddings (Eds.), *Field-Flow Fractionation Handbook*, John Wiley & Sons Inc., New York, 2000, p. 79.
- [26] M.R. Schure, K.D. Caldwell, J.C. Giddings, *Anal. Chem.* 58 (1986) 1509.
- [27] J. Chmelik, *J. Chromatogr. A* 845 (1999) 285.
- [28] J. Plockova, F. Matulik, J. Chmelik, *J. Chromatogr. A* 955 (2002) 95.
- [29] X. Tong, K.D. Caldwell, *J. Chromatogr. B* 674 (1995) 39.
- [30] P.S. Williams, S. Lee, J.C. Giddings, *Chem. Eng. Commun.* 130 (1994) 143.
- [31] M. Martin, P.S. Williams, *NATO ASI Ser., Ser. C* 383 (1992) 513.
- [32] S. You, S.G. Stevenson, M.S. Izydorczyk, K.R. Preston, *Cereal Chem.* 79 (2002) 624.
- [33] P. Reschiglian, A. Zattoni, S. Casolari, A. Krumlova, M. Budinska, J. Chmelik, *Ann. Chim.: Rome* 92 (2002) 457.
- [34] L. Farmakis, G. Karaiskakis, A. Koliadima, *J. Liq. Chromatogr. Relat. Technol.* 25 (2002) 2135.
- [35] C. Contado, F. Dondi, *Starch/Stärke* 53 (2001) 414.
- [36] J. Chmelik, A. Krumlova, M. Budinska, T. Kruml, V. Psota, I. Bohacenko, P. Mazal, H. Vydrova, *J. Inst. Brew.* 107 (2001) 11.
- [37] C. Contado, P. Reschiglian, S. Faccini, A. Zattoni, F. Dondi, *J. Chromatogr. A* 871 (2000) 449.
- [38] J. Chmelik, V. Psota, *Proc. Congr. Eur. Brew. Conv.* 27th (1999) 421.
- [39] M.H. Moon, J.C. Giddings, *J. Food Sci.* 58 (1993) 1166.
- [40] D. Clédat, S. Battu, R. Mokrini, P.J.P. Cardot, *J. Chromatogr. A* 1049 (2004) 131.
- [41] P. Cardot, S. Battu, A. Simon, C. Delage, *J. Chromatogr. B* 768 (2002) 285.
- [42] R. Sanz, P. Cardot, S. Battu, M.T. Galceran, *Anal. Chem.* 74 (2002) 4496.
- [43] C. Corbiere, S. Battu, B. Liagre, P.J.P. Cardot, J.L. Beneytout, *J. Chromatogr. B* 808 (2004) 255.
- [44] D.Y. Leger, B. Liagre, P.J.P. Cardot, J.L. Beneytout, S. Battu, *Anal. Biochem.* 335 (2004) 267.
- [45] P. Bernfeld, in: S.P. Colowick, N.O. Kaplan (Eds.), *Method Enzymol.*, Baltimore, 1955, p. 149.
- [46] S. Battu, A. Roux, S. Delebasee, C. Bosgiraud, P.J.P. Cardot, *J. Chromatogr. B* 751 (2001) 131.
- [47] S. Battu, J. Cook-Moreau, P.J.P. Cardot, *J. Liq. Chromatogr. Relat. Technol.* 25 (2002) 2193.
- [48] A. Gilman-Sachs, *Anal. Chem.* 66 (1994) 700A.
- [49] H.M. Shapiro, *Method Cell Biol.* 63 (2001) 107.
- [50] R.A. Hoffman, *Method Cell Biol.* 63 (2001) 299.
- [51] C.F. Bohren, D.R. Huffman, *Absorption and Scattering of Light by Small Particles*, John Wiley & Sons, New York, 1998.
- [52] P.J.P. Cardot, T. Chianea, S. Battu, in: J. Cazes (Ed.), *Encyclopedia of Chromatography*, M. Dekker Inc., New York, 2001, p. 742.
- [53] W. Helbert, M. Schulein, B. Henrissat, *Int. J. Bio. Macromol.* 19 (1996) 165.
- [54] N. Lindeboom, P.R. Chang, R.T. Tyler, *Starch/Stärke* 56 (2004) 89.
- [55] N.E. Assidjo, T. Chianea, I. Clarot, M.F. Dreyfuss, P.J.P. Cardot, *J. Chromatogr. Sci.* 37 (1999) 229.
- [56] B.N. Barman, J.C. Giddings, *Anal. Chem.* 67 (1995) 3861.
- [57] P.J.P. Cardot, J.-M. Launay, M. Martin, *J. Liq. Chromatogr. Relat. Technol.* 20 (1997) 2543.
- [58] J.C. Giddings, *Analyst* (Cambridge, UK) 118 (1993) 1487.
- [59] J.J. Kirkland, L.E. Schallinger, W.W. Yau, *Anal. Chem.* 57 (1985) 2271.
- [60] L. Koch, T. Koch, H.M. Widmer, *J. Chromatogr.* 517 (1990) 395.
- [61] M. Miller, Y. Jiang, M.E. Hansen, *Book of Abstracts*, 216th ACS National Meeting, Boston, 23–27 August 1998, AGFD.
- [62] S. Saenton, H. Lee, Y.-S. Gao, J.F. Ranville, S.K.R. Williams, *Sep. Sci. Technol.* 35 (2000) 1761.
- [63] R.V. Sharma, R.T. Edwards, R. Beckett, *Appl. Environ. Microbiol.* 59 (1993) 1864.
- [64] P. Reschiglian, D. Melucci, G. Torsi, *J. Chromatogr. A* 740 (1996) 245.
- [65] B.N. Barman, E.R. Ashwood, J.C. Giddings, *Anal. Biochem.* 212 (1993) 35.
- [66] Y.H. Park, D.W. Lee, M.H. Moon, *Instrum. Sci. Technol.* 25 (1997) 133.
- [67] W.-S. Kim, D.W. Lee, S. Lee, *Anal. Chem.* 74 (2002) 848.
- [68] R. Beckett, Y. Jiang, G. Liu, M.H. Moon, J.C. Giddings, *Part. Sci. Technol.* 12 (1994) 89.
- [69] P. Blau, R.L. Zollars, *J. Colloid Interface Sci.* 183 (1996) 476.
- [70] R. Beckett, J.C. Giddings, *J. Colloid Interface Sci.* 186 (1997) 53.